OCT-Based Retina Assessment Reflects Visual Impairment in Multiple Sclerosis

Natacha Stolowy,[1,2] Lilija Gutmann,[3] Margareta Lüpke,[3] Thierry David,[1,4] Michael Dorr,[5] Christina Mayer,[3] Christoph Heesen,[3] Frederike Cosima Oertel,[6–8] Ting-Yi Lin,[6,9] Friedemann Paul,[6–8] Hanna Gwendolyn Zimmermann,[6–8,10] and Jan-Patrick Stellmann[2,3,11]

[1]APHM, Hopital de la Conception, Department of Ophthalmology, Marseille, France
[2]Aix Marseille University, CNRS, CRMBM, Marseille, France
[3]Institute of Neuroimmunology and Multiple Sclerosis, University Medical Center Hamburg-Eppendorf, Hamburg, Germany
[4]Aix Marseille University, CNRS, Marseille, France
[5]Adaptive Sensory Technology, Lübeck, Germany
[6]Experimental and Clinical Research Center, Max Delbrück Center for Molecular Medicine and Charité - Universitätsmedizin Berlin, Corporate Member of Freie Universität Berlin and Humboldt-Universität zu Berlin, Berlin, Germany
[7]Neuroscience Clinical Research Center, Charité-Universitätsmedizin Berlin, Corporate Member of Freie Universität Berlin and Humboldt-Universität zu Berlin, Berlin, Germany
[8]Department of Neurology, Charité-Universitätsmedizin Berlin, Corporate Member of Freie Universität Berlin and Humboldt-Universität zu Berlin, Berlin, Germany
[9]Department of Neurology, Johns Hopkins University, Baltimore, Maryland, United States
[10]Einstein Center Digital Future, Berlin, Germany
[11]APHM, Hopital de la Timone, CEMEREM, Marseille, France

Correspondence: Natacha Stolowy, Assistance Publique-Hôpitaux de Marseille, Conception, 147 boulevard Baille, Marseille 13385, France; natacha.stolowy@ap-hm.fr.

Received: September 18, 2024
Accepted: January 14, 2025
Published: February 13, 2025

Citation: Stolowy N, Gutmann L, Lüpke M, et al. OCT-based retina assessment reflects visual impairment in multiple sclerosis. *Invest Ophthalmol Vis Sci.* 2025;66(2):39. https://doi.org/10.1167/iovs.66.2.39

Purpose. To explore the relationship between visual performance and retinal morphology as assessed by optical coherence tomography (OCT), and the ability of OCT to reflect visual impairment in people with multiple sclerosis (PwMS) compared with healthy controls (HC).

Methods. We gathered data from two neurology referral centers on PwMS and HC. Neurological and ophthalmological assessments, including OCT, high-contrast visual acuity (HCVA) and low-contrast visual acuity (LCVA), area under the log contrast sensitivity function (AULCSF), and vision-related quality of life (National Eye Institute Visual Function Questionnaire), were conducted between 2018 and 2020, with follow-up at 1 year.

Results. A total of 137 PwMS (271 eyes) and 118 HC (236 eyes) were available for analysis. The peripapillary retinal nerve fiber layer (pRNFL) and the macular ganglion cell layer and inner plexiform layer volume (mGCIPL) volume were both reduced in PwMS (92 µm in PwMS vs 98 µm in HC [$P < 0.001$], 0.55 mm^3 vs 0.62 mm^3 [$P < 0.001$], respectively). A cutoff effect for visual impairment was observed in PwMS when pRNFL fell below 68.8 µm (HCVA), 71.4 µm (LCVA), and 72.6 µm (AULCSF). Using mixed effects models, the mGCIPL volume emerged as the variable most strongly associated with the AULCSF ($P < 0.001$). The AULCSF showed the strongest correlation with both pRNFL and mGCIPL ($P < 0.001$), with optic neuritis being a significant contributing factor ($P < 0.001$).

Conclusions. AULCSF outperformed standard HCVA and LCVA, closely reflecting retinal atrophy. mGCIPL loss showed stronger associations with vision tests and detected neurodegeneration without the cutoff effect seen in pRNFL, making it the best marker for neuronal atrophy.

Keywords: multiple sclerosis, visual function, vision, contrast sensitivity function, visual acuity, retina, optical coherence tomography, controls

Multiple sclerosis (MS) is a chronic neuroinflammatory disease that can affect the visual system. Visual impairment is recognized as a common and extremely debilitating manifestation for individuals affected by MS.[1–3] Visual impairment can result from various mechanisms. The primary cause is the occurrence of optic neuritis, affecting approximately 20% of patients with MS as initial attack.[4] However, visual impairment can be present without any history of optic neuritis. Optic nerve atrophy may occur through a retrograde trans-synaptic mechanism secondary to damage to the downstream visual pathways in the brain.[5,6] This process is independent of inflammation and may also

occur in progressive MS with a predominantly neurodegenerative disease course and less inflammation.

Assessing the visual sequelae of people with MS (PwMS) is challenging in clinical practice because they are poorly evaluated by high-contrast visual acuity (HCVA). A study found persistent complaints related to visual symptoms in one-third of PwMS.[7] The vision-related quality of life questionnaire National Eye Institute Visual Function Questionnaire (NEI-VFQ) reveals the presence of persistent deficits related to vision 5 to 8 years after the occurrence of optic neuritis.[8] This condition was primarily attributed to the presence of bilateral optic neuritis or internuclear ophthalmoplegia. HCVA is often deemed good after the occurrence of optic neuritis. However, other measures provide a more accurate assessment of visual sequelae in PwMS, both with and without optic neuritis. The assessment of visual function using low-contrast charts, such as the Sloan chart or the Pelli–Robson chart, has been shown to be a robust and representative measure of visual function in individuals with MS. This sensitive measure exhibits a strong correlation with both quality of life and visual quality scores.[7,9–11] Even more precise is the complete contrast sensitivity function (CSF), which proves to be the most accurate measurement of visual function.[12] However, until recently, evaluating this curve was confined to the research field and was a laborious process. The Lesmes et al. team has introduced a swift and reliable measurement method for the CSF and the area under the log CSF (AULCSF), validated for PwMS in a computer-based format.[12–16] However, it is yet not well-explored how different vision tests relate to the underlying neuronal damage.

Optical coherence tomography (OCT) is an optimal tool for assessing retinal damage. It is known that OCT reveals abnormalities in PwMS. Involvement of the peripapillary retinal nerve fiber layer (pRNFL) is well-recognized: it seems to be normal or increased in the acute phase of optic neuritis and may progress to atrophy.[17] Anomalies in other retinal layers are also observed. Thinning of the ganglion cell–inner plexiform layer is noted, sometimes at the acute phase of optic neuritis or several months later,[18,19] and also in patients without ocular involvement.[20] Retinal degeneration can be observed in the earliest disease phase and is likely stable throughout the course of the disease.[21] However, the link between visual function and neuronal and retinal damage is not well-understood and some evidence indicates a nonlinear relationship between vision and retinal damage.[21]

The main objective of this study was to explore the relationship between visual function and retinal layer thicknesses and volumes as assessed by OCT, first by identifying the visual test most strongly correlated with retinal damage and second by investigating the ability of OCT to reflect visual impairment in PwMS compared with control subjects. The secondary objectives were to describe the visual function and retinal morphology of PwMS compared with healthy control (HC).

Methods

Participants

We gathered data from two neurology referral centers in Germany on patients diagnosed with MS (PwMS), as well as HC. Neurological and ophthalmological assessments were conducted in a prospective manner between 2018 and 2020 in Hamburg (center HH) and in Berlin (center B).

Patients included were diagnosed with MS based on the modified 2017 McDonald criteria,[22] including relapsing–remitting, primary progressive, and secondary progressive forms, with or without a history of optic neuritis. The collected data included demographic information (age, sex), disease type and its characteristics (year of initial symptom manifestation, year of formal diagnosis, diagnosis status, and immunotherapies), and history of optic neuritis. A subset of patients underwent follow-up assessments at 1 year after inclusion in the cohort.

HC had no history of ophthalmological or neurological conditions. They underwent a medical history interview and a neurological examination conducted by a neurologist. They were recruited to match the age distribution of PwMS.

Neurological and Ophthalmological Data

Neurological disability was assessed with the Expanded Disability Status Scale.[23] The relevant visual data analyzed for this study were high-contrast visual acuity (HCVA) using the Snellen chart at 5 m, distance HCVA using Sloan chart 100%, low-contrast visual acuity (LCVA) with the Sloan chart 2.5%, and the area under the log CSF (AULCSF). CSFs were assessed with the Manifold Contrast Vision Meter (Adaptive Sensory Technology, Inc, San Diego, CA, USA) that used the quantitative CSF algorithm to choose from Sloan letters between 0.2 and 100% contrast and from 1.5 to 40.0 cycles per degree to obtain an estimate of the CSF and to calculate the area under the log CSF. Visual tests were performed with best optical correction in Berlin and with habitual optical correction in Hamburg. The ophthalmological examination data were collected, including intraocular pressure, refraction data, and calculation of spherical equivalent. Additionally, the vision-related quality of life questionnaire NEI-VFQ,[24] including the neuro-ophthalmological section,[25,26] were assessed.

OCT scans were performed with the Spectralis SD- OCT (Heidelberg Engineering, Heidelberg, Germany; pupils not dilated, eye tracking). For measurement of the pRNFL, we used a ring scan around the optic nerve head (12°, 1536 A- scans, 16 $\leq$ automatic real time averaging $\leq$ 100) using the device internal segmentation module 6.0.14.0. A macular volume scan (25° $\times$ 30°, 61 B- scans, 768 A-scans per B- scan, 12 $\leq$ automatic real time $\leq$ 15) quantified the macular ganglion cell layer and inner plexiform layer volume (mGCIPL) and the macular inner nuclear layer (mINL). Scans not meeting the OSCAR- IB consensus criteria were excluded.[27] The SAMIRIX pipeline was used for intra- retinal layer segmentation of the macula scans and volumes were extracted in a 3 mm diameter cylinder around the fovea.[28] The intereye absolute difference (IEAD) was defined as the pRNFL asymmetry between the right and left eye in each subject, as described by Petzold et al.[29] It is well-known that pRNFL and macular layer thicknesses decrease with age.[30–32] However, the data regarding IEAD are contradictory, with some authors reporting an increase with age,[21,33] whereas others report a decrease.[34] Therefore, we investigated whether the IEAD was correlated with age and whether this could explain the observed differences.

Statistics

Statistical analyses were carried out using the R software (R version 4.3.1) and additional R-packages (*ggplot2*, *lmerTest*, *segmented*, and *effects* packages).[35–38] Continuous numeric variables at the subjects level (Table 1) were

Table 1. Demographic and Clinical Characteristics

	HC (n = 118; 236 Eyes)	PwMS (n = 137; 271 Eyes)	P Value
Age (years)	40.3 ± 12.8	42.7 ± 10.4	0.102
Female sex	84 (71.2%)	81 (59.1%)	0.082
Duration of disease since diagnosis (years)	–	8.1 ± 7.6	
Disease course			
RRMS	–	112 (81.8%)	
PPMS		11 (8%)	
SPMS		14 (10.2%)	
EDSS score	–	2.4 ± 1.5	
		median ± interquartile range, 2 ± 1.5	
History of optic neuritis	–	94/271 (34.8%)	
NEI-VFQ			
General health	79.85 ± 13.79	61.12 ± 21.36	<0.001*
General vision	82.30 ± 12.93	74.85 ± 16.71	<0.001*
Ocular pain	92.61 ± 10.72	82.67 ± 19.33	<0.001*
Near activities	94.12 ± 7.98	87.85 ± 13.37	<0.001*
Distance activities	96.36 ± 5.42	91.72 ± 10.97	<0.001*
Social functioning	98.84 ± 3.81	96.28 ± 8.82	0.003*
Mental health	94.48 ± 5.56	86.84 ± 14.53	<0.001*
Role difficulties	90.22 ± 12.67	80.82 ± 18.08	<0.001*
Dependency	99.78 ± 1.42	94.84 ± 14.38	<0.001*
Driving	86.26 ± 17.10	79.58 ± 25.44	<0.001*
Color vision	99.13 ± 4.60	98.85 ± 5.27	0.33
Peripheral vision	98.03 ± 6.77	90.84 ± 15.87	<0.001*
Neuro-ophthalmology	80.90 ± 25.53	63.51 ± 23.61	<0.001*

EDSS, expanded disability status scale; PPMS, primary progressive multiple sclerosis; RRMS, relapsing remitting multiple sclerosis; SPMS, secondary progressive multiple sclerosis.
* $P < 0.05$ (false discovery rate–adjusted P values for the NEI-VFQ).

described by the mean and standard deviation, except for Expanded Disability Status Scale score, which was described both by the mean and standard deviation and by the median and interquartile range. Discontinuous numeric variables and categorical variables were described in terms of count and frequency. Continuous numeric variables at the eyes level (Table 2, Supplementary Table S1) were described by the adjusted mean with a 95% confidence interval from linear mixed effect models adjusted for center effect, age, and sex.

After confirming the normal distribution of the data, parametric tests were used for comparisons of continuous quantitative variables (t-test for the comparison of HC and PwMS). The χ^2 test or Fisher's exact test were used for the comparison of categorical (qualitative) variables. The comparisons of HC eyes and PwMS eyes were based on linear mixed-effects models adjusted for center effect age and sex with the subject as random effect to adjust for inter-eye dependencies. A P value less than 0.05 was considered to be statistically significant after correction for multiple testing with false discovery rate. In the boxplots, the box represent the interquartile range from the first quartile (Q1) to the third quartile (Q3), with the line inside the box indicating the median. The whiskers extend to the smallest and largest values within 1.5 times the interquartile range from Q1 and Q3, respectively. Outliers beyond the whiskers are displayed as individual points. The y axis for HCVA values were inverted such as better vision is always represented at the top of the plots.

Bivariate and multiple correlation analyses were based on linear mixed effects models that allow to model unbalanced

Table 2. Ocular Characteristics: Data by Eyes, for Visit at Baseline and at the 1-Year Follow-Up Visit

		PwMS				
	HC (n = 290 Eyes)	Total (n = 313 Eyes)	No History of ON (n = 204 Eyes)	History of ON (n = 108 Eyes)	P Value: HC Vs. Total PwMS	P Value: PwMS Without Vs. With History of ON
Vision						
HCVA (LogMAR), adjusted mean	**−0.08 [−0.1; −0.06]**	**−0.04 [−0.06; −0.02]**	**−0.07 [−0.09; −0.04]**	**−0.01 [−0.05; 0.02]**	**0.006***	**0.016***
HCVA (Sloan 100%, letters)	**57.88 [56.89; 58.87]**	**55.91 [54.97; 56.84]**	56.85 [55.49; 58.21]	55.12 [53.34; 56.91]	**0.006***	0.11
LCVA (Sloan 2.5%, letters)	**34.16 [32.74; 35.57]**	**27.95 [26.61; 29.3]**	**30.84 [28.98; 32.69]**	**27.78 [25.36; 30.19]**	**<0.001***	**0.035***
AULCSF	**1.34 [1.3; 1.38]**	**1.22 [1.18; 1.25]**	**1.28 [1.23; 1.33]**	**1.18 [1.12; 1.24]**	**<0.001***	**0.003***
Eye examination						
Intraocular pressure	14.54 [13.44; 15.64]	13.86 [12.64; 15.08]	13.57 [12.7; 14.44]	13.47 [12.5; 14.45]	0.415	0.883
Spherical equivalent	−0.94 [−1.41; −0.48]	−0.55 [−1.08; −0.03]	**−0.19 [−0.72; 0.34]**	**−1.07 [−1.67; −0.46]**	0.278	**0.036***
OCT						
pRNFL thickness (µm)	**97.53 [95.33; 99.74]**	**92.36 [90.31; 94.42]**	**96.3 [93.94; 98.67]**	**82.64 [79.71; 85.57]**	**0.001***	**<0.001***
mGCIPL, volume (mm^3)	**0.62 [0.61; 0.63]**	**0.55 [0.54; 0.57]**	**0.58 [0.56; 0.59]**	**0.5 [0.48; 0.52]**	**<0.001***	**<0.001***
mINL, volume (mm^3)	0.29 [0.29; 0.3]	0.3 [0.29; 0.3]	**0.3 [0.29; 0.3]**	**0.3 [0.3; 0.31]**	0.108	**0.039***

ON, optic neuritis; pRNFL, peripapillary retinal nerve fiber layer.
Data are highlighted in bold and marked with an asterisk (*) for $P < 0.05$ (false discovery rate–adjusted P values).
Data as adjusted mean with a 95% confidence interval from linear mixed effect models adjusted for center effect, age and sex with the subject as random effect to adjust for inter-eye dependencies.

Investigative Ophthalmology & Visual Science

repeated measures experimental designs and adjusts for intereye dependencies.[39,40] The center effect was assessed throughout the analyses. For bivariate analyses, we standardized the variables (mean-centered and scaled to unit variance) prior to conducting the bivariate analyses to ensure that the beta estimates obtained from the model are comparable to Pearson correlation coefficients. Stepwise selection, in conjunction with the Akaike information criterion, was used to determine the most appropriate regression model (polynomial or linear) for the bivariate analyses. Segmented models were used to obtain cutoff effects in HC eyes. Stepwise selection, in conjunction with the Akaike information criterion and likelihood ratio tests, was used to assess an optimal random-effects structure in the multiple correlations. The significance of fixed effects in the model was assessed using P values.

Ethics

All patients and HC provided written informed consent. The study adhered to the Helsinki Declaration. The study was approved by the local ethics committee (Ethical Committee of the Board of Physicians Hamburg, PV5557, Ethical Committee of the Charité-Universitätsmedizin Berlin, EA1/163/12). Participants gave informed consent to participate in the study before taking part.

Results

A total of 137 PwMS (75 from center HH and 62 from center B) and 118 HC (86 from center HH and 32 from center B) were available for analysis. Demographic and clinical characteristics are summarized in Table 1. Some patients had follow-up visits: 21 PwMS and 27 HC were reviewed 1 year after inclusion. Both groups were comparable in terms of age, sex ratio, and ophthalmological examination (refraction and intraocular pressure). PwMS were comparable between both centers in term of age (42.9 in center HH vs 42.4 in center B, $P = 0.76$) and of disease course ($P = 0.49$)

Visual functions were reduced in center HH compared with center B (Fig. 1). The difference in refraction techniques may have contributed to these differences. In each center and in the total cohort, all visual functions were reduced in the MS group, with a significant difference for logMAR HCVA, LCVA, and AULCSF (Fig. 1; Table 2). Among PwMS, LCVA and AULCSF were significantly lower in those with a

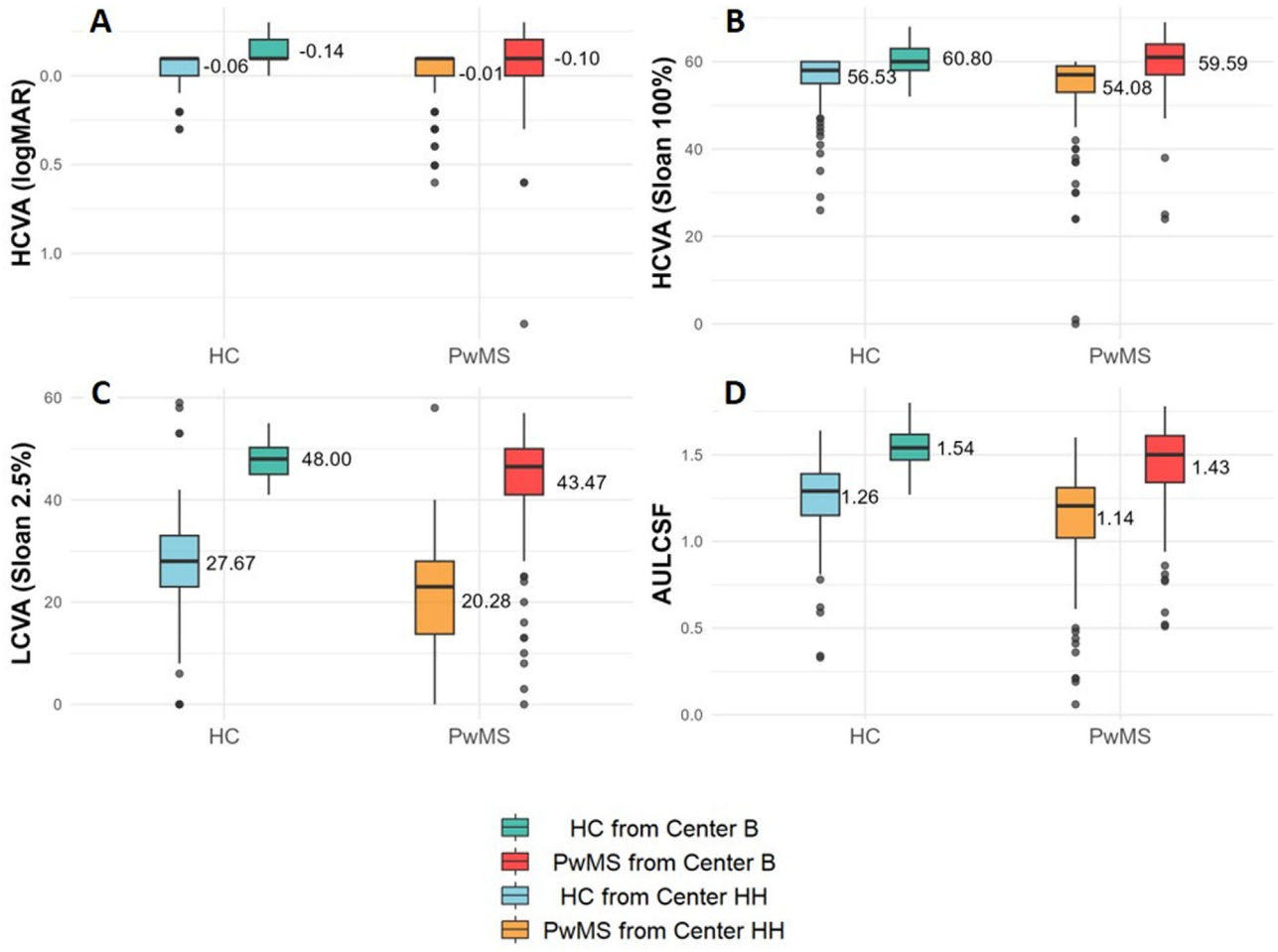

Figure 1. Comparison of visual functions between HC eyes ($n = 288$) and patients with MS eyes ($n = 310$). Boxplots with whiskers. The line inside the boxplot represents the median. The mean is represented by a diamond symbol, with the corresponding numeric value displayed. (**A**) HCVA in logMAR. (**B**) HCVA measured with the Sloan chart at 100% contrast. (**C**) LCVA measured with the Sloan chart at 2.5% contrast. (**D**) AULCSF.

Investigative Ophthalmology & Visual Science

history of optic neuritis (Table 2). Low performance at 2.5% contrast is very common. In fact, in our cohort, 15 PwMS (21 eyes) had an LCVA of zero. Among these patients, HCVA and AULCSF were not only measurable, but also discriminatory with a more refined distribution for AULCSF, demonstrating that this method is more informative and offers better classification than LCVA at 2.5% contrast (Fig. 2). The NEI-VFQ results indicated significantly diminished outcomes in the MS group across all subscales, except for color vision (Table 1).

The pRNFL was significantly lower in MS group versus HC. Total and sectoral mGCIPL were also significantly lower in the MS group. Total mINL and multiple sectors of the mINL were elevated in the MS group. Within the MS group, the pRNFL and all sectors of the mGCIPL were reduced in PwMS with a history of optic neuritis compared with those without. Notably, when comparing PwMS without a history of optic neuritis to HC, there was no significant difference in pRNFL ($P = 0.08$). However, all sectors of the mGCIPL were reduced in PwMS without a history of optic neuritis compared with HC ($P < 0.001$). Among PwMS, no significant difference in mGCIPL and in mINL was observed between the nasal and temporal sectors. Ocular characteristics are summarized in Table 2 and Supplementary Table S1 and shown in Figure 3.

The IEAD was higher in PwMS compared with HC (7.92 ± 9.06 µm vs 2.78 ± 2.52 µm; $P < 0.001$). The IEAD was not correlated with age in either subgroup ($P = 0.76$ in MS, 0.33 in HC, Fig. 3E). It was higher in patients with a history of unilateral optic neuritis compared with patients without a known history (Fig. 3F).

Among the HC, 54 eyes from 27 HC were evaluated at the 1-year follow-up. There were no significant changes in HCVA, LCVA, AULCSF, pRNFL, mGCIPL, or mINL. Furthermore, these parameters remained unchanged in the 42 eyes of 21 PwMS who were reassessed at the 1-year follow-up (Supplementary Fig. S1).

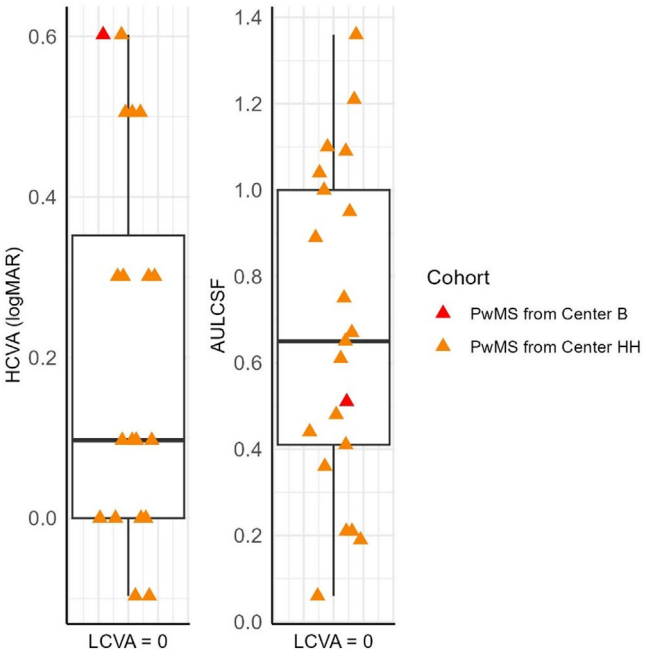

Figure 2. HCVA and AULCSF values in eyes with a LCVA (Sloan 2.5%) at zero. The *y* axis for HCVA values inverted such as better vision is always represented at the top of the plots.

In PwMS, visual parameters were correlated with pRNFL and mGCIPL volume. A cutoff effect, that is the average point when further retinal atrophy cannot be compensated anymore and loss of visual functioning occurs, was observed when pRNFL fell below 68.83 µm (HCVA), 71.42 µm (LCVA), and 72.64 µm (AULCSF) (Fig. 4). The mGCIPL volume did not exhibit this threshold effect, and the correlation was linear for all visual parameters (Fig. 4). The beta-estimates of bivariate associations were −0.35 ($P < 0.001$), 0.45 ($P < 0.001$), and 0.56 ($P < 0.001$) between the mGCIPL volume and HCVA, LCVA, and AULCSF respectively. There was no significant correlation between the mINL and the various visual tests: the beta-estimates were 0.07 ($P = 0.06$), −0.08 ($P = 0.13$), and −0.08 ($P = 0.1$) between mINL volume and HCVA, LCVA, and AULCSF, respectively.

Next, we examined which retinal outcome correlates with visual function best. The results of the mixed effects model are presented in Table 3. The mGCIPL volume was the most closely associated with AULCSF, with a significant fixed effect. History of optic neuritis was not associated significantly with visual function. Finally, we aimed to determine which visual outcome is the most indicative of retinal damage. When performing multiple regression analyses with OCT outcomes as the dependent variables, the best correlated vision test for pRNFL and mGCIPL was the AULCSF and history of optic neuritis was also a significant explanatory factor (Table 4).

Discussion

Our study aimed to identify an optimized selection of vision and OCT outcomes to monitor visual function loss and its underlying neurodegeneration in a large cohort of patients with MS and HC. From a visual function perspective, the complete CSF outperforms standard HCVA and LCVA assessments, because it was more closely related to retinal atrophy and remains highly informative in patients with no vision on the LCVA charts. Concerning OCT outcomes, mGCIPL loss showed a closer association with all vision tests and detects neurodegeneration, even in eyes without previous optic neuritis. Moreover, mGCIPL has no cutoff effect, in contrast with pRNFL. Thus, mGCIPL loss directly translates into visual impairment supporting mGCIPL as the best parameter to monitor neuronal atrophy independent from clinical inflammatory episodes.

When searching for the best visual test to indicate cellular loss on OCT with mixed effects models, the only visual test correlated with both the pRNFL and the mGCIPL volume was the AULCSF. The history of optic neuritis was also significant. These two factors were not significant for the mINL. Thus, we robustly demonstrate the usefulness of the AULCSF in assessing PwMS. Because contrast sensitivity varies with spatial frequency, the full CSF—which assesses spatial resolution at all contrast levels—is a highly valuable measure of vision in psychophysics and physiology. Visual acuity, whether tested at high contrast or different levels of low contrast, represents only a single point on this contrast sensitivity curve. Also, contrast sensitivity is associated with cognitive performance such as information processing speed and memory.[41] However, to date, a comprehensive CSF assessment has not been feasible for multicenter trials or clinical routine owing to lengthy examination times. The device used for this study has been explored and validated previously[12–16] and

Investigative Ophthalmology & Visual Science

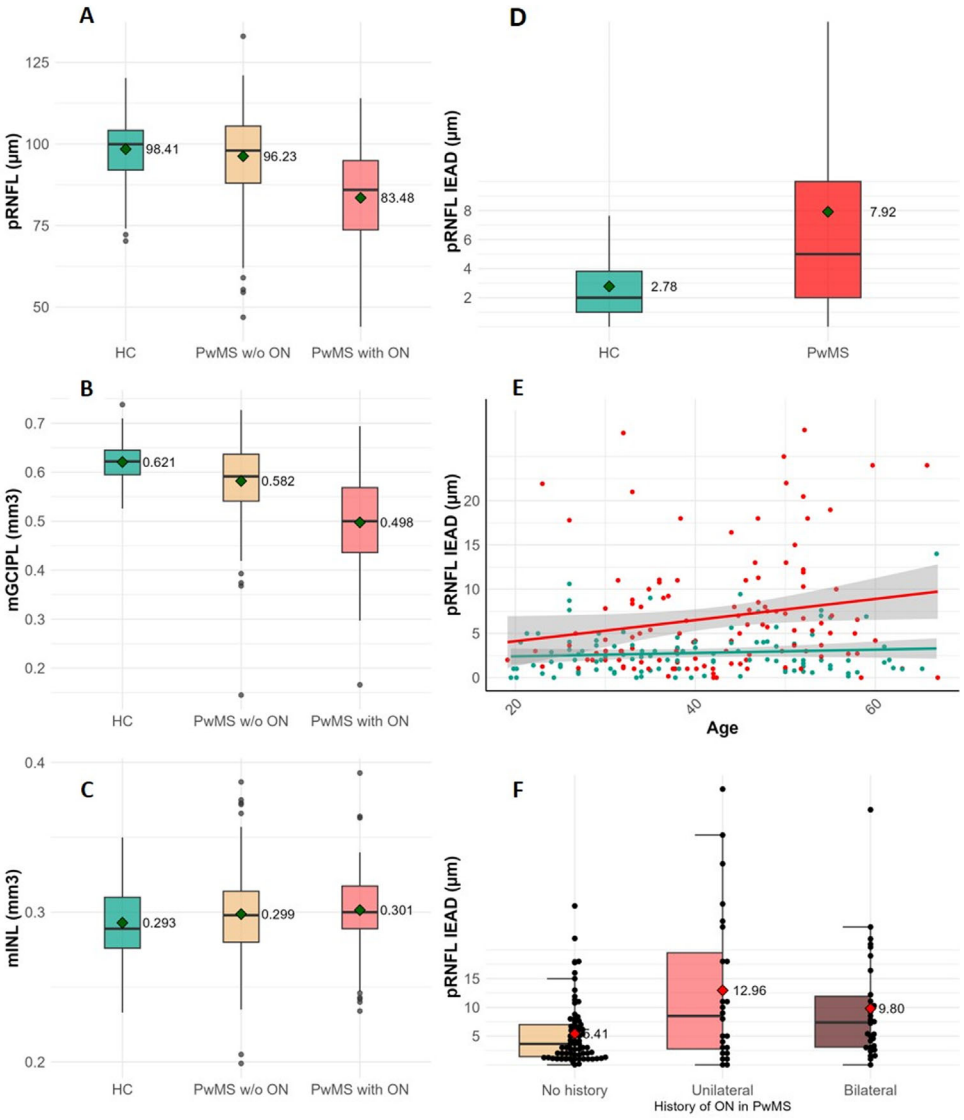

Figure 3. OCT profile. (**A**) Comparison of pRNFL between HC eyes, PwMS eyes without optic neuritis (w/o ON), and PwMS with ON. (**B**) Comparison of mGCIPL between HC eyes, PwMS eyes without optic neuritis and PwMS with ON. (**C**) Comparison of mINL between HC eyes, PwMS eyes without ON, and PwMS with ON. (**D**) Comparison of IEAD between PwMS and HC. (**E**) Scatter plot of the IEAD against the age. HC, *green*; PwMS, *red*. (**F**) Comparison of IEAD of PwMS depending on the history of ON.

allows for rapid and highly reproducible measurement of the AULCSF. As shown in Table 2, the AULCSF was significantly reduced in PwMS (total, with optic neuritis) compared with HC. Furthermore, among PwMS in which we observe a floor effect (LCVA at zero), the AULCSF exhibits excellent variability and serves as a tool to discriminate between patients and allowing a better individual follow-up, which aligns with the results of Rosenkranz et al.[16]

Mixed effect models also identified the retinal layer most associated to each visual parameter, namely the mGCIPL. The correlation of the mGCIPL with each visual parameter was linear and significant for each visual parameter. It was already described for HCVA, LCVA, and visual evoked potential,[42–44] but rarely for AULCSF. It seems that the mGCIPL is more sensitive than pRNFL and is strongly correlated with visual function, because early mGCIPL loss is not detectable by pRNFL. Indeed, a cutoff effect is observed when correlating the pRNFL with each visual parameter, indicating a decline in visual function when the pRNFL falls below approximately 73 µm. This effect explains the preservation of vision even in the presence of optic atrophy, as described by Rosenkranz et al.,[21] and explains why the pRNFL is not the best marker for assessing the risk of visual loss. This effect was previously observed by Costello et al.,[17] who noted visual field deterioration when the pRNFL dropped below 75 µm. This threshold was higher (approximately 90 µm) in Rosenkranz et al.,[21] likely because it was analyzed in patients with primary progressive MS, who exhibit less inflammatory optic nerve involvement compared with the relapsing-remitting MS patients, who are predominant in our cohort. We observed a cutoff effect with HCVA, LCVA, and AULCSF (with a more sensitive cutoff) in two independent cohorts and in comparison with HC, which demonstrates strong evidence of this phenomenon. Therefore, it seems that cell loss translates more closely in the mGCIPL, a phenomenon well-established in glaucoma[45,46]

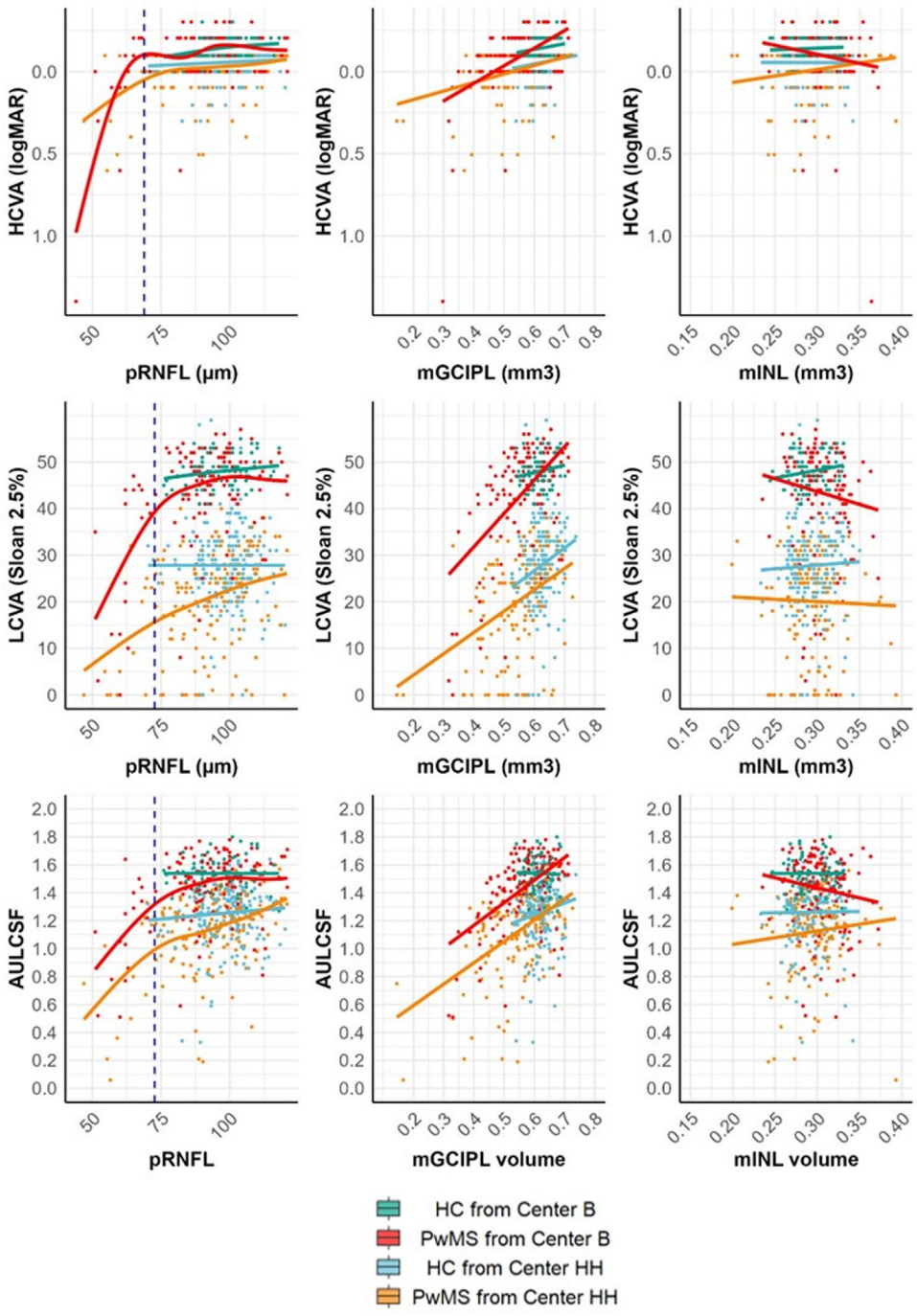

Figure 4. Scatter plots of visual parameters as a function of OCT parameters. The *solid lines* represent polynomial regression for the plots against pRNFL (*column 1*) and linear regression for the other columns (*column 2 and column 3*). In the *first column* (plots against pRNFL), the *dashed line* indicates the cutoff of the segmented model. PwMS are represented in *green* (center B) and *blue* (center HH), whereas HC are represented in *red* (center B) and *orange* (center HH). In center HH, visual tests were conducted with the subject's habitual optical correction. In center B, visual tests were best- corrected visual tests. The *y* axis for HCVA values inverted such as better vision is always represented at the top of the plots.

and recently described in intracranial hypertension,[47] but less understood in MS.[48,49] This finding can be explained partly by the anatomical distribution of ganglion cells and retinal nerve fiber, which makes an early modification less visible at the level of the neuroretinal ring compared with the macular region, where the cellular layers are more spread out and distributed according to the retinal sector. Additionally, some authors propose that astrogliosis, primarily occurring in the RNFL, could lead to an erroneous increase in pRNFL thickness.[18,44] The presence of astrogliosis might compromise the precision of OCT in measuring RNFL thickness compared with mGCIPL measurements. This discrepancy could potentially explain the better structure–function correlations observed with mGCIPL thickness than pRNFL thickness.[18,44] Interestingly, adaptive optics have provided new insights into retinal lesions in PwMS at a cellular

Investigative Ophthalmology & Visual Science

Table 3. Mixed Effect Models for Each Visual Outcome Measure: HCVA, LCVA, and AULCSF

	HCVA (logMAR)				LCVA (2.5%)				AULCSF			
	Full Model		Stepwise Selection of Variables		Full Model		Stepwise Selection of Variables		Full Model		Stepwise Selection of Variables	
Dependent Variable	Estimates ± SE	*P* Value	Estimates ± SE	*P* Value	Estimates ± SE	*P* Value	Estimates ± SE	*P* Value	Estimates ± SE	*P* Value	Estimates ± SE	*P* Value
Intercept	**0.32 ± 0.16**	**0.044***	**0.35 ± 0.06**	**<0.001***	**19.92 ± 9.72**	**0.044***	**25.3 ± 8.23**	**0.002***	0.48 ± 0.25	0.056	**0.43 ± 0.09**	**<0.001***
Age (decade)	−0.002 ± 0.01	0.835	–	–	0.37 ± 0.72	0.605	–	–	0.02 ± 0.02	0.317	–	–
Male sex	0.004 ± 0.02	0.875	–	–	−0.85 ± 1.57	0.587	–	–	−0.02 ± 0.04	0.676	–	–
Center HH	**0.09 ± 0.02**	**<0.001***	**0.08 ± 0.02**	**<0.001***	**−23.62 ± 1.49**	**<0.001***	**−23.13 ± 1.45**	**<0.001***	**−0.31 ± 0.04**	**<0.001***	**−0.29 ± 0.04**	**<0.001***
History of ON	−0.01 ± 0.02	0.611	–	–	1.45 ± 1.48	0.33	–	–	0.03 0.03	0.408	–	–
pRNFL	0	0.192	–	–	0.04 ± 0.07	0.513	–	–	0	0.783	–	–
mGCIPL volume	**−0.65 ± 0.17**	**<0.001***	**−0.8**	**<0.001***	**59.02 ± 10.31**	**<0.001***	**61.02 ± 6.59**	**<0.001***	**1.78 ± 0.24**	**<0.001***	**1.76 ± 0.15**	**<0.001***
mINL volume	0.28 ± 0.42	0.506	–	–	−50.51 ± 25.94	0.053	**−53.39 ± 24.35**	**0.03***	−0.56 ± 0.64	0.383	–	–

ON, optic neuritis; SE, standard error.
Data are highlighted in bold and marked with an asterisk (*) for $P < 0.05$.

Table 4. Mixed Effect Models for Each OCT Outcome Measure: pRNFL, mGCIP Volume, and mINL Volume

	pRNFL				mGCIPL Volume				mINL Volume			
	Full Model		Stepwise Selection of Variables		Full Model		Stepwise Selection of Variables		Full Model		Stepwise Selection of Variables	
Dependent Variable	Estimates ± SE	*P* Value	Estimates ± SE	*P* Value	Estimates ± SE	*P* Value	Estimates ± SE	*P* Value	Estimates ± SE	*P* Value	Estimates ± SE	*P* Value
Intercept	**54.57 ± 13.92**	**<0.001***	**45.81 ± 13.02**	**<0.001***	**0.38 ± 0.04**	**<0.001***	**0.33 ± 0.02**	**<0.001***	**0.31 ± 0.01**	**<0.001***	**0.32 ± 0.01**	**<0.001***
Age (decade)	−1.67 ± 0.98	0.092	–	–	−0.01 ± 0.01	0.068	–	–	0	0.253	–	–
Male sex	16 ± 12.42	0.199	17.49 ± 12.41	0.16	−0.01 ± 0.01	0.677	–	–	0.01 ± 0.005	0.089	–	–
Center HH	**9.93 ± 2.47**	**<0.001***	**8.51 ± 2.14**	**<0.001***	**0.05 ± 0.01**	**<0.001***	**0.05 ± 0.01**	**<0.001***	**−0.02 ± 0.005**	**0.003***	**−0.02 ± 0.01**	**0.002***
History of ON	**−11.41 ± 1.48**	**<0.001***	**−11.64 ± 1.48**	**<0.001***	**−0.05 ± 0.01**	**<0.001***	**−0.06 ± 0.01**	**<0.001***	0	0.242	–	–
AULCSF	**15.75 ± 4.23**	**<0.001***	**18.57 ± 2.44**	**<0.001***	**0.16 ± 0.03**	**<0.001***	**0.17 ± 0.02**	**<0.001***	−0.01 ± 0.01	0.34	–	–
HCVA	0.54 ± 6.21	0.931	–	–	0.01 ± 0.04	0.72	–	–	−0.01 ± 0.01	0.06	–	–
LCVA	0.1 ± 0.09	0.302	–	–	0	0.37	–	–	0	0.093	**− 0.0002 ± 0.00005**	**0.007**

ON, optic neuritis.
Data are highlighted in bold and marked with an asterisk (*) for $P < 0.05$.

level. Hargrave et al.[50] identified novel signs visible on the macula of PwMS in both reflectance confocal and split-detection adaptive optics scanning laser ophthalmoscopy images, which they described as scattering features. These scattering features appear to be specific to MS, and their number and surface area were associated with HCVA and LCVA in these patients, showing stronger correlations than with pRNFL. Their pathophysiological significance remains uncertain, but they may correspond with microglial cells, immune cells, hyalocytes, or inanimate elements resulting from phagocytosing microglia or degenerating neurites in Henle's fiber layer in a context or neuroretinal inflammation. Hammer et al.[51] also reported modifications of the macular retina observed with adaptive optics. Their images revealed a 51% decrease in the density of retinal ganglion cells in PwMS compared with HC and an increase in the size of residual cells. They also observed an increased density of macrophage cells in the ILM that might explain the absence of significant changes in this layer in PwMS. The association found between adaptive optics and the GCL and IPL on OCT suggests that thinning of the mGCIPL is largely a direct consequence of retinal ganglion cell loss, which is consistent with previous studies.[52,53] Our findings provide new insights into the understanding of visual loss in PwMS with or without optic neuritis and underscores the importance of regular monitoring and systemic treatment to slow disease progression and reduce the risk of optic neuritis relapse, to avoid falling below this cellular threshold, which would lead to a dramatic decrease in vision.

Given that the age and disease course of PwMS were comparable between center HH and center B, the differences observed between the centers can likely be attributed to the use of optical correction. Higher results were obtained in center B, where patients used optimized optical correction during visual testing. Another limitation that could explain the observed differences is the possible variations in lighting and distance within the testing room. Even under differing refractive techniques, similar slopes and effects were observed across both centers. This finding confirms the reproducibility of the observed phenomena and strongly supports the robustness of these findings. In clinical practice, best possible optical correction should always be put on to optimize visual function independent from neuronal damage in the visual system.

Regarding the secondary objectives of the study, our results confirm visual impairment across all visual parameters in PwMS compared with HC. Visual impairment was more pronounced in cases with a history of optic neuritis, but there was still a significant difference between PwMS without optic neuritis and HC. Indeed, the visual decline in MS is due to mechanisms affecting the afferent pathways of the visual system at various levels, not just the optic nerve, and also the efferent pathways of the visual system.[2] Retrograde trans-synaptic degeneration is a process in which the degeneration of postsynaptic neurons triggers degenerative changes in presynaptic neurons connected to them, propagating backward along neural pathways. It plays a key role in PwMS and explains possible retinal loss and consequent involvement of visual function, even in the absence of direct optic nerve inflammation.[6,52] Vision is one of the first functions affected in PwMS[1] and it is well-known that the NEI-VFQ is reduced in PwMS.[7,10] Our results demonstrate a decrease in nearly all NEI-VFQ-25 subscales compared with HC.

The limitations of the study are primarily the heterogeneous composition of the MS cohort and the slightly different setups at the twocenters with a divergent optic correction strategy. The history of optic neuritis was analyzed, which is essential for understanding the retinal function and anatomy in PwMS. However, the number of optic neuritis episodes and the duration between optic neuritis and the examination were not analyzed owing to significant missing data. Furthermore, a longitudinal study could introduce a temporal factor to enhance the understanding of cellular loss over time and over repeated optic neuritis episodes.

Conclusions

This study supports the combination of AULCSF and mGCIPL as the best outcome set to monitor visual function in PwMS. AULCSF proves to be a precise tool not only for assessing vision, but also for pointing to cellular loss in the retina. The mGCIPL measurement by OCT is vice versa a reliable marker of visual function global evaluation, unlike pRNFL, which can miss early signs of visual loss. AULCSF and mGCIPL have the potential to guide treatment decisions on an individual level with the chance to decrease the risk for serious visual complications in PwMS.

Acknowledgments

Data acquisition in Hamburg was partially supported by an unrestricted grant from Genzyme.

Disclosure: **N. Stolowy**, None; **L. Gutmann**, None; **M. Lüpke**, None; **T. David**, None; **M. Dorr**, Financial and intellectual property interest in contrast sensitivity function assessment; **C. Mayer**, None; **C. Heesen**, Biogen (F, R, S), Celgene (F, R, S), Genzyme (F, R, S), Merck and Roche (F, R, S), all outside of this work; **F.C. Oertel**, Hertie foundation (F), Novartis and DFG-TWAS program (F), not related to this project, Past fellowship support by the American Academy of Neurology and the National MS Society. Past research grant by the DGN (Germany Neurology Association), UCB (S), Guthy Jackson Charitable Foundation (R), European Committee for Research and Treatment in Multiple Sclerosis (ECTRIMS) and American Academy of Neurology (AAN) (R), Academic Section Editor at DGNeurologie; **T.-Y. Lin**, None; **F. Paul**, German Ministry for Education and Research (BMBF) (F), Deutsche Forschungsgemeinschaft (DFG) (F), Einstein Foundation (F), Guthy Jackson Charitable Foundation (F), EU FP7 Framework Program (F), Biogen (F), Genzyme (F), Merck Serono (F), Novartis (F), Bayer (F), Roche (F), all unrelated to this project, Consulting fees by Alexion, Roche, Horizon, Neuraxpharm. Almirall (S), Bayer (S), Biogen (S), GlaxoSmith-LKline (S), Heal (S), Merck (S), Sanofi Genzyme (S), Novartis (S), Viela Bio (S), UCB (S), Mitsubishi Tanabe (S), Celgene (S), Guthy Jackson Foundation (S), Serono and Roche (S), Merck (R), Guthy Jackson Foundation (R), Bayer (R), Biogen (R), Merck Serono (R), Sanofi Genzyme (R), Novartis (R), Alexion (R), Viela Bio (R), Roche (R), UCB (R), Mitsubishi Tanabe (R), Celgene (R), Celgene (S), Roche (S), UCB (S), AdBoard for Merck (S), Academic Editor at *PLoS One* and *Neurology, Neuroimmunology and Neuroinflammation*; **H.G. Zimmermann**, Novartis (F), unrelated to this project; **J.-P. Stellmann**, None

References

1. Heesen C, Böhm J, Reich C, et al. Patient perception of bodily functions in multiple sclerosis: gait and visual function are the most valuable. *Mult Scler J*. 2008;14(7):988–991.

2. Balcer LJ, Miller DH, Reingold SC, et al. Vision and vision-related outcome measures in multiple sclerosis. *Brain*. 2015;138(1):11–27.
3. Heesen C, Haase R, Melzig S, et al. Perceptions on the value of bodily functions in multiple sclerosis. *Acta Neurol Scand*. 2018;137(3):356–362.
4. Costello F. The afferent visual pathway: designing a structural-functional paradigm of multiple sclerosis. *ISRN Neurol*. 2013;2013:134858.
5. Gabilondo I, Martínez-Lapiscina EH, Martínez-Heras E, et al. Trans-synaptic axonal degeneration in the visual pathway in multiple sclerosis. *Ann Neurol*. 2014;75(1):98–107.
6. Petracca M, Cordano C, Cellerino M, et al. Retinal degeneration in primary-progressive multiple sclerosis: a role for cortical lesions? *Mult Scler J*. 2017;23(1):43–50.
7. Jasse L, Vukusic S, Durand-Dubief F, et al. Persistent visual impairment in multiple sclerosis: prevalence, mechanisms and resulting disability. *Mult Scler J*. 2013;19(12):1618–1626.
8. Cole SR, Beck RW, Moke PS, Gal RL, Long DT. The National Eye Institute Visual Function Questionnaire: experience of the ONTT. Optic Neuritis Treatment Trial. *Invest Ophthalmol Vis Sci*. 2000;41(5):1017–1021.
9. Baier ML, Cutter GR, Rudick RA, et al. Low-contrast letter acuity testing captures visual dysfunction in patients with multiple sclerosis. *Neurology*. 2005;64(6):992–995.
10. Mowry EM, Loguidice MJ, Daniels AB, et al. Vision related quality of life in multiple sclerosis: correlation with new measures of low and high contrast letter acuity. *J Neurol Neurosurg Psychiatry*. 2009;80(7):767–772.
11. Balcer LJ, Raynowska J, Nolan R, et al. Validity of low-contrast letter acuity as a visual performance outcome measure for multiple sclerosis. *Mult Scler J*. 2017;23(5):734–747.
12. Lesmes LA, Lu ZL, Baek J, Albright TD. Bayesian adaptive estimation of the contrast sensitivity function: the quick CSF method. *J Vis*. 2010;10(3):17.1–21.
13. Dorr M, Lesmes LA, Lu ZL, Bex PJ. Rapid and reliable assessment of the contrast sensitivity function on an iPad. *Invest Ophthalmol Vis Sci*. 2013;54(12):7266–7273.
14. Kalia A, Lesmes LA, Dorr M, et al. Development of pattern vision following early and extended blindness. *Proc Natl Acad Sci U S A*. 2014;111(5):2035–2039.
15. Stellmann J, Young K, Pöttgen J, Dorr M, Heesen C. Introducing a new method to assess vision: computer-adaptive contrast-sensitivity testing predicts visual functioning better than charts in multiple sclerosis patients. *Mult Scler J - Exp Transl Clin*. 2015;1:2055217315596184.
16. Rosenkranz SC, Kaulen B, Zimmermann HG, et al. Validation of computer-adaptive contrast sensitivity as a tool to assess visual impairment in multiple sclerosis patients. *Front Neurosci*. 2021;15:591302. Accessed December 1, 2023. https://www.frontiersin.org/articles/10.3389/fnins.2021.591302
17. Costello F, Coupland S, Hodge W, et al. Quantifying axonal loss after optic neuritis with optical coherence tomography. *Ann Neurol*. 2006;59(6):963–969.
18. Green AJ, McQuaid S, Hauser SL, et al. Ocular pathology in multiple sclerosis: retinal atrophy and inflammation irrespective of disease duration. *Brain J Neurol*. 2010;133(Pt 6):1591–1601.
19. Syc SB, Saidha S, Newsome SD, et al. Optical coherence tomography segmentation reveals ganglion cell layer pathology after optic neuritis. *Brain J Neurol*. 2012;135(Pt 2):521–533.
20. Ratchford JN, Saidha S, Sotirchos ES, et al. Active MS is associated with accelerated retinal ganglion cell/inner plexiform layer thinning. *Neurology*. 2013;80(1):47–54.
21. Rosenkranz SC, Gutmann L, Has Silemek AC, et al. Visual function resists early neurodegeneration in the visual system in primary progressive multiple sclerosis. *J Neurol Neurosurg Psychiatry*. 2023;94(11):924–933.
22. Thompson AJ, Banwell BL, Barkhof F, et al. Diagnosis of multiple sclerosis: 2017 revisions of the McDonald criteria. *Lancet Neurol*. 2018;17(2):162–173.
23. Kurtzke JF. Rating neurologic impairment in multiple sclerosis: an expanded disability status scale (EDSS). *Neurology*. 1983;33(11):1444–1452.
24. Mangione CM, Lee PP, Gutierrez PR, et al. Development of the 25-item National Eye Institute Visual Function Questionnaire. *Arch Ophthalmol Chic Ill 1960*. 2001;119(7):1050–1058.
25. Raphael BA, Galetta KM, Jacobs DA, et al. Validation and test characteristics of a 10-item neuro-ophthalmic supplement to the NEI-VFQ-25. *Am J Ophthalmol*. 2006;142(6):1026–1035.
26. Wagenbreth C, Sabel BA, Tönnies S, et al. [The neuroophthalmic supplement to the NEI-VFQ: test statistics and validation with a cohort of patients with pre- and postchiasmatic damage]. *Klin Monatsbl Augenheilkd*. 2011;228(11):971–978.
27. Tewarie P, Balk L, Costello F, et al. The OSCAR-IB consensus criteria for retinal OCT quality assessment. *PloS One*. 2012;7(4):e34823.
28. Motamedi S, Gawlik K, Ayadi N, et al. Normative data and minimally detectable change for inner retinal layer thicknesses using a semi-automated OCT image segmentation pipeline. *Front Neurol*. 2019;10:1117.
29. Petzold A, Chua SYL, Khawaja AP, et al. Retinal asymmetry in multiple sclerosis. *Brain*. 2021;144(1):224–235.
30. Sung KR, Wollstein G, Bilonick RA, et al. Effects of age on optical coherence tomography measurements of healthy retinal nerve fiber layer, macula, and optic nerve head. *Ophthalmology*. 2009;116(6):1119–1124.
31. Chen CY, Huang EJC, Kuo CN, et al. The relationship between age, axial length and retinal nerve fiber layer thickness in the normal elderly population in Taiwan: The Chiayi eye study in Taiwan. Paul F, ed. *PloS One*. 2018;13(3):e0194116.
32. Ooto S, Hangai M, Tomidokoro A, et al. Effects of age, sex, and axial length on the three-dimensional profile of normal macular layer structures. *Invest Ophthalmol Vis Sci*. 2011;52(12):8769–8779.
33. Al-Haddad C, Antonios R, Tamim H, Noureddin B. Interocular symmetry in retinal and optic nerve parameters in children as measured by spectral domain optical coherence tomography. *Br J Ophthalmol*. 2014;98(4):502–506.
34. Tao Y, Tham Y, Chee M, et al. Profile of retinal nerve fibre layer symmetry in a multiethnic Asian population: the Singapore Epidemiology of Eye Diseases study. *Br J Ophthalmol*. 2019;104:836–841.
35. R Core Team. *R: A language and environment for statistical computing*. Vienna, Austria: R Foundation for Statistical Computing; 2018.
36. Wickham H. *Ggplot2*. New York: Springer International Publishing; 2016.
37. Kuznetsova A, Brockhoff PB, Christensen RHB. lmerTest package: tests in linear mixed effects models. *J Stat Softw*. 2017;82:1–26.
38. Fox J, Weisberg S. *An R companion to applied regression*. Thousand Oaks, CA: SAGE Publications; 2018.
39. Bolker BM, Brooks ME, Clark CJ, et al. Generalized linear mixed models: a practical guide for ecology and evolution. *Trends Ecol Evol*. 2009;24(3):127–135.
40. Cheng J, Edwards LJ, Maldonado-Molina MM, Komro KA, Muller KE. Real longitudinal data analysis for real

Investigative Ophthalmology & Visual Science

people: Building a good enough mixed model. *Stat Med*. 2010;29(4):504–520. Published online 2009:n/a-n/a.

41. Wieder L, Gäde G, Pech LM, et al. Low contrast visual acuity testing is associated with cognitive performance in multiple sclerosis: a cross-sectional pilot study. *BMC Neurol*. 2013;13:167.
42. Walter SD, Ishikawa H, Galetta KM, et al. Ganglion cell loss in relation to visual disability in multiple sclerosis. *Ophthalmology*. 2012;119(6):1250–1257.
43. Narayanan D, Cheng H, Tang RA, et al. Multifocal visual evoked potentials and contrast sensitivity correlate with ganglion cell-inner plexiform layer thickness in multiple sclerosis. *Clin Neurophysiol Off J Int Fed Clin Neurophysiol*. 2019;130(1):180–188.
44. Saidha S, Syc SB, Durbin MK, et al. Visual dysfunction in multiple sclerosis correlates better with optical coherence tomography derived estimates of macular ganglion cell layer thickness than peripapillary retinal nerve fiber layer thickness. *Mult Scler J*. 2011;17(12):1449–1463.
45. Kim YK, Ha A, Na KI, et al. Temporal relation between macular ganglion cell–inner plexiform layer loss and peripapillary retinal nerve fiber layer loss in glaucoma. *Ophthalmology*. 2017;124(7):1056–1064.
46. Marshall HN, Andrew NH, Hassall M, et al. Macular ganglion cell–inner plexiform layer loss precedes peripapillary retinal nerve fiber layer loss in glaucoma with lower intraocular pressure. *Ophthalmology*. 2019;126(8):1119–1130.
47. Attia R, Fitoussi R, Mairot K, et al. Risk factors associated with progression from papilloedema to optic atrophy: results from a cohort of 113 patients. *BMJ Open Ophthalmol*. 2023;8(1):e001375.
48. Huang-Link YM, Al-Hawasi A, Lindehammar H. Acute optic neuritis: retinal ganglion cell loss precedes retinal nerve fiber thinning. *Neurol Sci*. 2015;36(4):617–620.
49. Behbehani R, Abu Al-Hassan A, Al-Salahat A, et al. Optical coherence tomography segmentation analysis in relapsing remitting versus progressive multiple sclerosis. *PloS One*. 2017;12(2):e0172120.
50. Hargrave A, Sredar N, Khushzad F, et al. Novel foveal features associated with vision impairment in multiple sclerosis. *Invest Ophthalmol Vis Sci*. 2021;62(12):27.
51. Hammer DX, Kovalick K, Liu Z, et al. Cellular-level visualization of retinal pathology in multiple sclerosis with adaptive optics. *Invest Ophthalmol Vis Sci*. 2023;64(14):21.
52. Quinn TA, Dutt M, Shindler KS. Optic neuritis and retinal ganglion cell loss in a chronic murine model of multiple sclerosis. *Front Neurol*. 2011;2:50.
53. Kanamori A, Catrinescu MM, Traistaru M, et al. In vivo imaging of retinal ganglion cell axons within the nerve fiber layer. *Invest Ophthalmol Vis Sci*. 2010;51(4):2011–2018.